J Therm Anal Calorim (2012) 109:883–892
DOI 10.1007/s10973-011-1784-2

Synthesis, spectroscopic, thermal characterization, and antimicrobial activity of miconazole drug and its metal complexes

Hanan F. Abd El-Halim · F. A. Nour El-Dien · Gehad G. Mohamed · Nehad A. Mohamed

Received: 9 May 2011 / Accepted: 29 June 2011 / Published online: 24 July 2011

Abstract Metal complexes having the general composition $[MCl_2(H_2O)_2(L)_2]\cdot yH_2O$ (where $y = 1$–3, M = Mn(II), Cu(II), Co(II), Ni(II), and Zn(II) and L = miconazole drug = MCNZ) and $[MCl_2(H_2O)_2(L)_2]Cl\cdot 3H_2O$ (where M = Cr(III) and Fe(III)) have been synthesized. All the synthesized complexes were identified and confirmed by elemental analyses, IR, diffused reflectance, and thermal analyses (TG and DTA) techniques as well as molar conductivity and magnetic moment measurements. The molar conductance data reveals that bivalent metal complexes are non-electrolytes while Cr(III) and Fe(III) complexes are electrolytes and of 1:1 type. IR spectral studies reveal that MCNZ is coordinated to the metal ions in a neutral unidentate manner with N donor site of the imidazole-*N*. On the basis of magnetic and solid reflectance spectral studies, an octahedral geometry has been assigned for the complexes. Detailed studies of the thermal properties of the complexes were investigated by thermogravimetry (TG) and differential thermal analyses (DTA) techniques and the activation thermodynamic parameters are calculated using Coats–Redfern method. The free MCNZ drug and its complexes were also evaluated against bacterial species (*P. aeruginosa*, *S. aureus*, *B. subtilis*, *E. Coli*) and fungi (*A. fumigatus*, *P. italicum*, *and C. albicans*) in vitro. The activity data show that the metal complexes have higher biological activity than the parent MCNZ drug.

H. F. Abd El-Halim (✉)
Department of Pharmaceutical Chemistry, Faculty of Pharmacy, Misr International University, Cairo, Egypt
e-mail: hanan.farouk2@yahoomail.com

F. A. Nour El-Dien · G. G. Mohamed · N. A. Mohamed
Department of Chemistry, Faculty of Science, Cairo University, Giza 12613, Egypt

Keywords Miconazole · Metal complexes · Spectroscopic studies · Thermal analyses · Biological activity

Introduction

Metallopharmaceuticals playing a significant role in therapeutic and diagnostic medicine, the discovery and development of new metallodrugs remain an ever growing area of research in medicinal inorganic chemistry [1–3].

Imidazole and other azole ring systems are structural features of many drugs and natural products [4, 5]. Azoles are typically susceptible to *N*-alkylation, forming azolium cations [3]. Many of the latter undergo deprotonation of a ring C–H R to the nitrogen, generating an azolidene carbine [6]. In at least one case, that of thiamine (vitamin B1), such a carbene is thought to be involved in the biological function of the molecule [6–9]. In turn, the capacity of azolidene carbenes to function as ligands in transition-metal complexes is well-established [10, 11]. Consequently, biologically relevant molecules containing azoles are candidates as carbine sources for metal complexation. We consider the utilization of drugs or natural products in this role to have a potential and useful approach in the development of new compounds used in medicinal and biochemical applications. Further, since *N*-methylation is a common metabolic event [12–14]. Studies of such molecules may ultimately provide new insights into possible modes of metal-azole interactions in biological systems [15–17].

Metallic silver, silver salts, and silver complexes have been used in a variety of applications like water purification, wound management, eye-drops, anti-infective coatings in medical devices and in burn treatment because they

have potent antimicrobial properties but with low human toxicity [18–24]. Also they represent novel group of antifungal agents with potential applications for the control of fungal infections. Treatment of fungal cells with the Cu (II) and Ag (I) complexes resulted in a reduced amount of ergosterol in the cell membrane and subsequent increase in its permeability [25–27].

However, in this study metal complexes of Mn(II), Cr(III), Fe(III), Co(II), Ni(II), Cu(II), and Zn (II) transition metals with MCNZ drug molecule were prepared.

This new complexes are linked a drug-based ligand to a metal via a metal-nitrogen bond, and they complement a small family of antifungal drug-metal conjugates possessing metal-nitrogen linkages [28].

The solid complexes are characterized using different physico-chemical methods like elemental analyses (C, H, N, Cl, and metal content), IR, magnetic moment and reflectance spectra, and thermal analyses (TGA and DTA). Biological activities of the complexes are studied. The structure of the drug is given in Fig. 1.

Experimental section

Materials

All chemicals used were of the analytical reagent grade (AR), and of highest purity available. They included miconazole (Union P.Goup); $CuCl_2{\cdot}2H_2O$ (Prolabo); $CoCl_2{\cdot}6H_2O$ and $NiCl_2{\cdot}6H_2O$ (BDH); $ZnCl_2{\cdot}2H_2O$ (Ubichem), $CrCl_3{\cdot}6H_2O$ (Sigma); $MnCl_2{\cdot}2H_2O$, and $FeCl_3{\cdot}6H_2O$ (Prolabo). Organic solvent used was absolute ethyl alcohol. De-ionized water collected from all glass equipments was usually used in all preparations.

Instruments

Elemental microanalyses of the separated solid chelates for C, H, N, and Cl were performed at the Microanalytical Center, Cairo University. Infrared spectra were recorded on a Perkin-Elmer FT–IR type 1,650 spectrophotometer in wavenumber region 4000–400 cm^{-1}. The spectra were recorded as KBr pellets. The mass spectrum of the drug under investigation was recorded by EI technique at 70 eV using MS-5988 GS–MS Hewlett-Packard instrument at the Microanalytical Center, Cairo University. The thermal analyses (TG, DTG, and DTA) analyses were carried out in dynamic nitrogen atmosphere (20 mL min^{-1}) with a heating rate of 10 °C min^{-1} using Shimadzu TG-60H and DTA-60H thermal analyzers. The solid reflectance spectra were measured on a Shimadzu 3101pc spectrophotometer. The molar magnetic susceptibility was measured on powdered samples using the Faraday method. The diamagnetic corrections were made by Pascal's constant and Hg [$Co(SCN)_4$] was used as a calibrant.

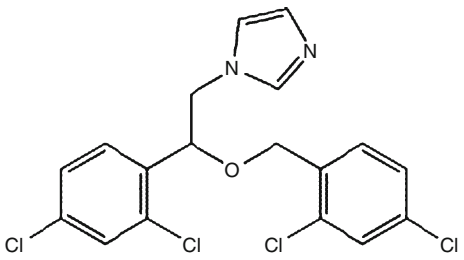

Fig. 1 Structure of MCNZ drug

Synthesis of metal complexes

Hot ethanolic solution (60 °C) of the appropriate metal chloride (1 mmol) in an ethanol–water mixture (1:1, 25 mL) was added to 25 mL of MCNZ (0.5 g, 2 mmol) hot ethanolic solution (60 °C). The resulting mixture was stirred under reflux for 1 h whereupon the complexes precipitated. They were collected by filtration, purified by washing several times with a 1:1 ethanol: water mixture and petroleum ether. The analytical data for C, H, N, and Cl were repeated twice.

Biological activity

The ligand and its corresponding metal complexes were screened in vitro for their antimicrobial activities against Bacterial strains (*Pseudomnas aeruginosa*, *Staphylococcus aureous, Bacillus subtilis, Escherichia coli*) and fungi strains (*Aspergillus fumigates, Penicillium italicum, Synephalastrum racemosum, and Candida albicans*) using agar well diffusion method. The samples were dissolved in DMSO to make a concentration of 100 µg/mL ligand and complexes and 2 mg/mL for standards. The inoculum (1×10^8 Cfu/mL) was added to molten agar and the media were shaken to disperse the microorganisms. Four millimeters diameter wells were punched in the agar with a sterile cork borer. 10 µl of the sample was introduced in the well. Antimicrobial activity was evaluated by measuring the diameter of inhibition zone in mm. The experiments were conducted in triplicate [29–31].

Results and discussion

The formation of metal complexes with organic compounds has long been recognized. However, the binary complexes of the cited drug with metal ions have not been studied yet, although they may be an area of interest. This is because they may affect the bioavailability of these drugs

as certain metal ions were present in relatively appreciable concentration in biological fluids.

The different pathways of the possible fragments of MCNZ with its respective relative intensities (RI) are given in Scheme 1. Fragment at $m/z = 414$ (RI = 100%) represents the base peak of MCNZ. The order molecular ion peaks appeared in the mass spectrum is attributed to the fragmentation obtained from the rupture of different bonds inside the drug molecule.

Composition and structures of metal complexes

The metal ions and MCNZ ligand was condensed in the ratio of 1:2 for the preparation of mononuclear complexes. The isolated solid complexes of Cr(III), Mn(II), Fe(III), Co (II), Ni (II), Cu (II), and Zn (II) were investigated by elemental analyses (C, H, N, Cl, and metal content), IR, magnetic moment studies, molar conductance, and thermal analyses (TG and DTA). The results of elemental analyses listed in Table 1 suggest that they have the composition $[MCl_2\ (H_2O)_2(L)_2]\cdot yH_2O$ (where $y = 1$ for M = Mn(II) or $y = 2$ for M = Cu(II), Co(II)), and $y = 3$ for M = Ni(II), Zn(II), and $[MCl_2(H_2O)_2(L)_2]Cl\cdot 3H_2O$ (where M = Cr(III) and Fe(III)). The results obtained are agreed well with the proposed formulae.

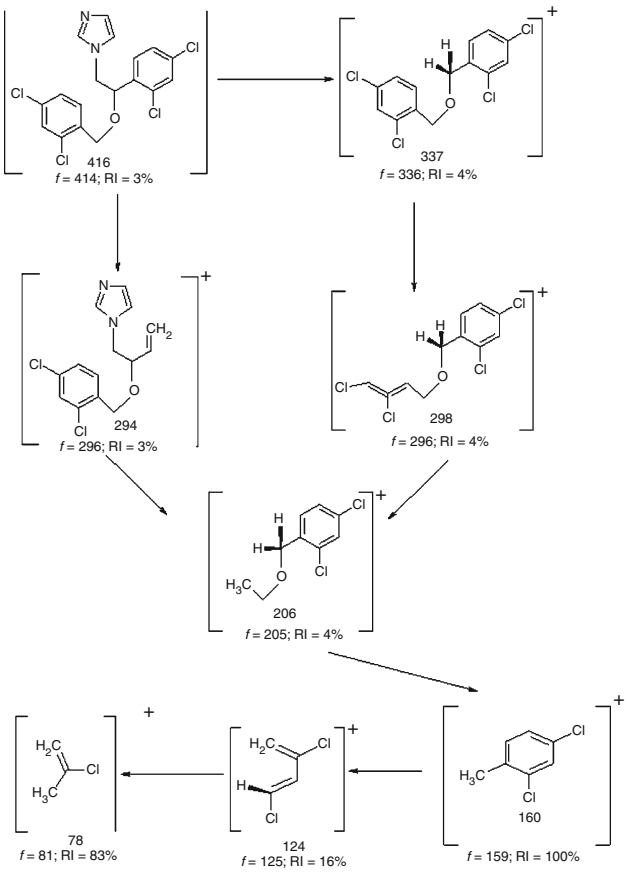

Scheme 1 Mass fragmentation pattern of MCNZ drug

Molar conductivity measurements

The conductance measures the ability of an aqueous solution to carry an electric current. It is concluded from the results that the complexes of the bivalent metal ions were found to have molar conductance values of 13–23 Ω^{-1} mol^{-1} cm^2, which indicates the non-ionic nature of these complexes and they are considered as non-electrolytes [32]. While for Cr(III) and Fe(III) complexes, the molar conductance values indicate the ionic nature of these complexes and they are of the type 1:1 electrolytes.

IR spectral studies and mode of bonding

The IR spectral data of the MCNZ drug and its metal complexes are listed in Table 2. The position and/or the intensities of these bands are expected to be changed upon chelation. These characteristic bands are listed in Table 2. Upon comparison it is found that the band located at 1631 cm^{-1} is assigned to the ν(C=N) stretching vibration of imidazole nitrogen for MCNZ drug [32]. Coordination of the imidazole nitrogen to the metal ion is indicated by a 3–9 and 4–23 cm^{-1} shift to lower and higher wave numbers, respectively. The band located at 1088 cm^{-1} is assigned to the ν(C–O–C) in the free drug. This band remains intact in solid complexes, indicating its non-involvement in coordination to the metal ions. The bands located at 3376–3550 and 907–964 cm^{-1} are assigned to the stretching vibrations of the hydrated and coordinated water molecules, respectively. The structural formula of the drug under investigation shows that it is promising in forming metal chelates through the *N* of the imidazole ring. According to IR data, it is concluded that MCNZ drug behaves as a neutral unidentate ligand coordinated to the metal ions via the imidazole *N*.

Magnetic susceptibility and electronic spectra measurements

From the diffused reflectance spectrum, it is observed that, the Fe(III) complex exhibits band at 20820 cm^{-1}, which may be assigned to the $^6A_{1g} \rightarrow T_{2g}(G)$ transition in octahedral geometry of the complexes. The $^6A_{1g} \rightarrow {}^5T_1g$ transition appears to be split into two bands at 16950 and 14650 cm^{-1}. The observed magnetic moment of the Fe(III) complex is 5.82 BM [33]. Thus, the complex formed has the octahedral geometry. The spectrum shows also band at 27690 cm^{-1} which may attributed to ligand to metal charge transfer.

Table 1 Analytical and physical data of MCNZ metal complexes

Complex	Color/% yield	M.p./°C	% Found (Calcd.)					μ_{eff}/BM	Λ_m/Ω^{-1}/mol/cm^2
			C	H	N	Cl	M		
$[CrCl_2(L)_2(H_2O)_2]Cl{\cdot}3H_2O$	Green	>300	39.86	3.33	5.59	35.95	4.18	5.80	92
$C_{36}H_{38}Cl_{11}CrN_4O_7$	(70)		(40.01)	(3.54)	(5.18)	(36.09)	(4.15)		
$[MnCl_2(L)_2(H_2O)_2]{\cdot}H_2O$	Buff	>300	42.80	3.32	5.47	15.12	5.43	5.61	23
$C_{36}H_{34}Cl_{10}MnN_4O_5$	(75)		(42.72)	(3.36)	(5.53)	(14.82)	(5.44)		
$[FeCl_2(L)_2(H_2O)_2]Cl{\cdot}3H_2O$	Brown	>300	40.11	3.12	5.47	36.33	5.15	5.82	86
$C_{36}H_{38}Cl_{11}FeN_4O_7$	(65)		(39.87)	(3.53)	(5.17)	(35.96)	(5.18)		
$[CoCl_2(L)_2(H_2O)_2]{\cdot}2H_2O$	Blue	>300	38.95	3.57	5.84	34.28	5.69	5.52	14
$C_{36}H_{36}Cl_{10}CoN_4O_6$	(68)		(39.15)	(3.48)	(5.41)	(34.33)	(5.71)		
$[NiCl_2(L)_2(H_2O)_2]{\cdot}3H_2O$	Yellow	>300	40.78	3.66	4.98	34.01	5.58	3.80	21
$C_{36}H_{38}Cl_{10}NiN_4O_7$	(60)		(41.10)	(3.63)	(5.33)	(33.70)	(5.58)		
$[CuCl_2(L)_2(H_2O)_2]{\cdot}2H_2O$	Green	>300	41.39	2.17	5.14	38.95	6.12	2.05	13
$C_{36}H_{36}Cl_{10}CuN_4O_6$	(85)		(41.67)	(2.47)	(5.39)	(39.24)	(6.13)		
$[ZnCl_2(L)_2(H_2O)_2]{\cdot}3H_2O$	Brown	>300	40.95	3.43	5.67	33.28	6.18	Diam.	21
$C_{36}H_{38}Cl_{10}N_4O_7Zn$	(80)		(40.84)	(3.62)	(5.29)	(33.49)	(6.17)		

Table 2 IR spectral data (4000–400 cm^{-1}) of the MCNZ drug and its metal complexes

Compound	ν(O–H) Hydrated water	ν(C=N)	ν(O–H) Coordinated water	ν(C–O–C)	ν(C–Cl)	ν(M–N)
MCNZ; L	–	1631m	–	1088m	1013m	–
$[CrCl_2(L)_2(H_2O)_2]Cl{\cdot}3H_2O$	3382m	1628m	954w	1088sh	1015m	438m
$[MnCl_2(L)_2(H_2O)_2]{\cdot}H_2O$	3419b	1628sh	964sh	1087m	1012m	439sh
$[FeCl_2(L)_2(H_2O)_2]Cl{\cdot}3H_2O$	3384b	1626m	907w	1091m	1010w	432m
$[CoCl_2(L)_2(H_2O)_2]{\cdot}2H_2O$	3550sh	1635sh	934m	1090sh	1040w	433m
$[NiCl_2\ (L)_2(H_2O)_2]{\cdot}3H_2O$	3376b	1628sh	963m	1088m	1013m	439sh
$[CuCl_2(L)_2(H_2O)_2]{\cdot}2H_2O$	3448b	1622w	953m	1088sh	1014m	433m
$[ZnCl_2(L)_2(H_2O)_2]{\cdot}3H_2O$	3403b	1654w	952sh	1099sh	1013m	436m

sh sharp, *m* medium, *s* small, *w* weak, *br* broad

The diffused reflectance spectrum of the Mn(II) complex displays four medium intensity bands at 15562, 18530, 21739, and 25340 cm^{-1} assignable to $^6A_{1g} \rightarrow {}^4T_{1g}({}^4G)$, $^6A_{1g} \rightarrow {}^4E_g$, $^6A_{1g} \rightarrow {}^4E_g({}^4D)$, and $^6A_{1g} \rightarrow {}^4T_{1g}({}^4P)$ transitions [33, 34]. The magnetic moment recorded at room temperature is found to be 5.61 BM corresponding to five unpaired electrons in octahedral geometry [35]. The diffused reflectance of the Co(II) complex with the general formula $[CoCl_2(L)_2(H_2O)_2]{\cdot}2H_2O$, gives three bands at 15550, 17820, and 19683 cm^{-1}, which are assigned to the transitions $^4T_{1g}$ (F) $\rightarrow {}^4T_{2g}$ (F) (ν_1), $^4T_{1g}$ (F) $\rightarrow {}^4A_{2g}$ (F) (ν_2) and $^4T_{1g}$ (F) $\rightarrow {}^4T_{2g}$ (P) (ν_3), respectively, suggesting that the Co(II) complex has octahedral geometry [36, 37].

The diffused reflectance spectra of the Cr(III) chelate exhibit bands at 21341–23730 which may be assigned to the $^6A_{1g} \rightarrow T_{2g}(G)$ transition in octahedral geometry of the complex. The observed magnetic moments of Cr(III) complex are 5.16, 5.47 BM The spectra show also bands at 25281–27645 cm^{-1} which may be attributed to ligand to metal charge transfer [37].

The diffused reflectance of the Ni (II) complex (beside the π–π^* and n–π^* bands of free drug) display three bands at ν_1: 15770 cm^{-1}: $^3A_{2g} \rightarrow {}^3T_{2g}$; ν_2: 19250 cm^{-1}: $^3A_{2g} \rightarrow {}^3T_{1g}$ (F), and ν_3: 22350 cm^{-1}: $^3A_{2g} \rightarrow {}^3T_{1g}$(P). The spectrum shows also a band at 25390 cm^{-1} which may attributed to ligand to metal charge transfer.

The magnetic moment values for Co (II) and Ni (II) complexes indicate the high-spin octahedral nature of the complexes [34–37].

The reflectance spectrum of Cu (II) complex exhibits a band at 14777 cm^{-1} which is assigned to the transition $^2E_g/{}^2T_{2g}$ in an octahedral geometry [34–37]. The magnetic moment of 2.05 BM falls within the range normally observed for octahedral Cu (II) complex. A moderately intense peak observed in the range 21555 cm^{-1} is due to ligand to metal charge transfer transition.

The Zn (II) complex is diamagnetic and an octahedral geometry was proposed based on its empirical formula.

Thermal analyses (TG, DTG, and DTA)

The TG curve of MCNZ (Fig. 2a) exhibits an estimated mass loss of 24.82% (calcd. 24.85%) within the temperature range 50–250 °C, which may be attributed to the liberation of $C_3H_3N_2$ and HCl molecules as gases. In the second and third stages within the temperature range 250–700 °C, the remaining part; $C_{15}H_{10}Cl_3O$ molecule is lost with an estimated mass loss of 75.18% (calcd. 75.12%) with a complete decomposition as CO, CO_2, NO, NH_3, etc., gases.

The thermal curve of the $[FeCl_2\ (L)_2(H_2O)_2]Cl{\cdot}3H_2O$ complex (Fig. 2b) shows four decomposition steps within the temperature range 30–700 °C. The first step of decomposition is found to be within the temperature range 30–100 °C which corresponds to the loss of water molecules of hydration with a mass loss of 4.39% (calcd. 4.98%). The energy of activation is found to be 31.02 kJ mol^{-1}. In the second stage within the temperature range 100–230 °C, the weight loss found may the decomposition of 3HCl molecules with a mass loss of 10.61% (calcd. 10.10%). The subsequent steps (230–700 °C) correspond to the removal of the two ligand molecules and $½H_2$ leaving metal oxide as a residue. The overall weight loss amounts to 91.39% (calcd. 91.09%).

The TG curves of the Cu(II) (Fig. 2c) and Co(II) (Fig. 2d) complexes show from three to four decomposition steps within the temperature range of 30–800 °C. The stages at 30–400 °C of the Cu(II) complex or 30–450 °C for Co(II) complex correspond to the loss of $3H_2O$, 2HCl, and $C_{14}H_8Cl_4O$ molecules. The energy of activation for these steps is 54.80 and 86.03 and 12.85 kJ mol^{-1} for Cu(II) and Co(II) complexes, respectively. While the subsequent stages involve the loss of $C_{22}H_{20}Cl_4N_4O$ molecule (as shown in Table 3), with a mass loss of 48.18% (calcd. 47.95%) and 48.03% (calcd. 48.16%) for Cu(II) and Co(II) complexes, respectively. The overall weight loss amounts to 93.04% (calcd. 92.34%) and 92.69% (calcd. 92.72%) for Cu(II) and Co(II) complexes, respectively.

Mn(II) complex is thermally decomposed in four decomposition steps, Fig. 2e, within the temperature range 30–700 °C. The first decomposition step with an estimated mass loss of 22.58% (calcd. 22.75%) within the

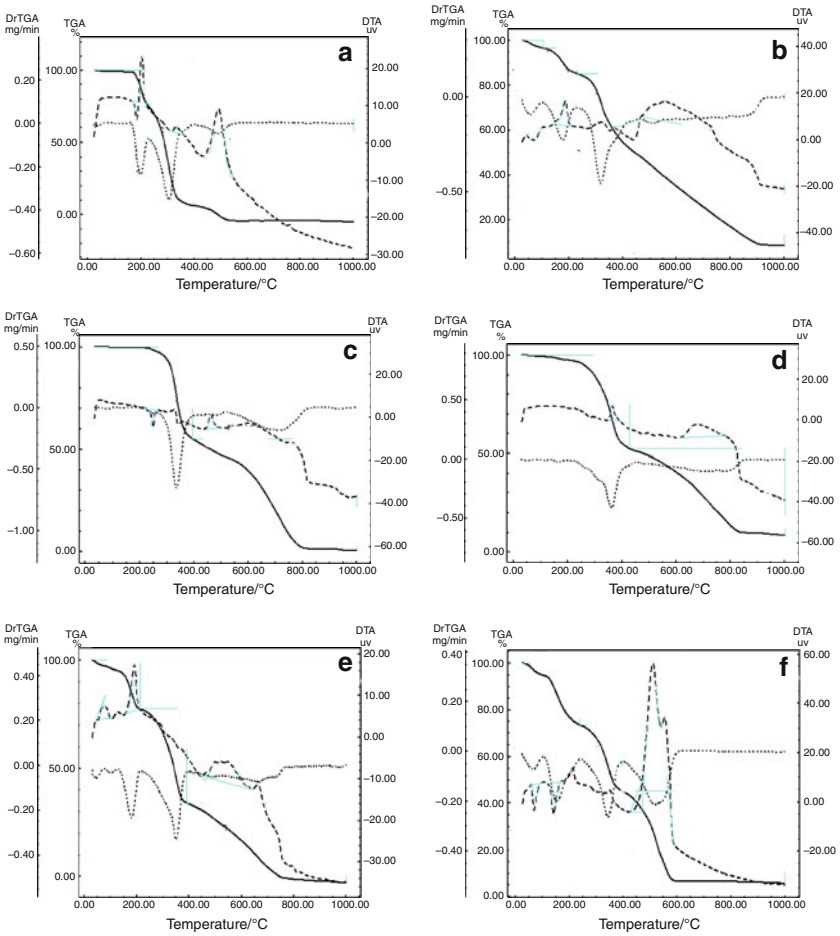

Fig. 2 Thermal analyses of (a) MCNZ drug (b) Fe(III) (c) Cu(II) (d) Co(II) (e) Mn(II) and (f) Ni(II) complexes

Table 3 Thermal analyses (TG, DTG, and DTA) data of MCNZ drug and its metal complexes

Compound	TG range/°C	*n*	Mass loss Total mass loss	%Found (calcd)	Assignment	Metallic residue	DTA/°C[a]
MCNZ; L	50–250	1	24.82 (24.85)	100 (99.97)	Loss of $C_3H_3N_2$ and HCl	–	163(+), 200(−), 230(+), 348(−), 433(+), 522(−)
	250–700	2	75.18 (75.12)		Loss of $C_{15}H_{10}Cl_3O$		
$[MnCl_2(L)_2(H_2O)_2]\cdot H_2O$	30–220	2	22.58 (22.75)	93.22 (93.06)	Loss of 2HCl, $2H_2O$ and $C_4H_2Cl_2$	MnO	100(−), 133(−), 219(−), 393(+), 450(−), 620(+), 669(−)
	220–395	1	41.54 (41.34)		Loss of $C_{20}H_{19}Cl_2\ N_4O_2$		
	395–700	1	29.19 (28.97)		Loss of $C_{12}H_7Cl_4$		
$[FeCl_2(L)_2(H_2O)_2]Cl\cdot 3H_2O$	30–100	1	4.39 (4.98)	91.39 (91.09)	Loss of $3H_2O$	$½Fe_2O_3$	53(−), 100(−), 176(−), 317(−), 430(+), 550(−)
	100–230	1	10.61 (10.10)		Loss of 3HCl		
	230–700	2	76.39 (76.01)		Loss of 2L -1½O and½H_2		
$[CoCl_2(L)_2(H_2O)_2]\cdot 2H_2O$	30–450	2	44.66 (44.58)	92.69 (92.72)	Loss of $3H_2O$, 2HCl and $C_{14}H_8Cl_4O$	CoO	300(−), 363(−), 500(−), 660(−)
	450–800	1	48.03 (48.16)		Loss of $C_{22}H_{20}Cl_4\ N_4O$		
$[Ni\ Cl_2\ (L)_2(H_2O)_2]\cdot 3H_2O$	25–250	2	27.48 (27.66)	93.12 (93.23)	Loss of $4H_2O$, 2HCl and $C_6H_3Cl_2$	NiO	28(+), 65(−), 160(−), 240(+), 345(+), 400(−), 527(+)
	250–400	1	32.04 (32.40)		Loss of $C_{15}H_{14}Cl_2O\ N_4$		
	400–700	1	33.60 (33.17)		Loss of $C_{15}H_{11}Cl_4\ O$		
$[CuCl_2(L)_2(H_2O)_2]\cdot 2H_2O$	30–400	2	44.86 (44.39)	93.04 (92.34)	Loss of $3H_2O$, 2HCl and $C_{14}H_8Cl_4O$	CuO	250(+), 266(−), 336(+), 450(−), 524.8(−)
	400–800	2	48.18 (47.95)		Loss of $C_{22}H_{20}Cl_4\ N_4O$		

n = number of decomposition steps

[a] (+) = endothermic, (−) = exothermic

Table 4 The antibacterial and antifungal activity of MCNZ drug and its metal complexes

Compound	mgmL^{-1}	*Aspergillus fumigatus*	*Penicillium italicum*	*Syncephalastrum racemosum*	*Candida albicans*	*Staphylococcus aureus*	*Pseudomonas aeruginosa*	*Bacillus subtilis*	*Escherichia coli*
MCNZ	1	0	0	0	0	+	0	+	0
	2.5	0	0	0	++	+	0	+	0
	5	0	0	0	++	+	+	+	0
$[CrCl_2(L)_2(H_2O)_2]Cl{\cdot}3H_2O$	1	0	0	0	0	+	0	+	0
	2.5	+	0	0	+	+	0	+	0
	5	+	+	0	+	+	0	+	0
$[MnCl_2(L)_2(H_2O)_2]{\cdot}H_2O$	1	0	0	0	+	+	0	+	0
	2.5	0	0	0	++	+	0	+	0
	5	0	0	0	++	+	0	+	0
$[FeCl_2(L)_2(H_2O)_2]Cl{\cdot}3H_2O$	1	0	0	0	0	+	0	++	0
	2.5	+	+	0	0	+	0	++	0
	5	+	+	0	0	+	0	++	+
$[CoCl_2(L)_2(H_2O)2]{\cdot}2H_2O$	1	0	0	0	+	+	0	+	0
	2.5	0	0	0	+	+	0	+	0
	5	0	0	0	+	+	0	+	0
$[NiCl_2(L)_2(H2O)_2]{\cdot}3H_2O$	1	0	0	0	+	+	0	+	0
	2.5	0	0	0	++	+	0	++	0
	5	0	0	0	++	+	0	++	0
$[CuCl_2(L)_2(H_2O)_2]{\cdot}2H_2O$	1	0	0	0	+	+	0	+	0
	2.5	0	0	0	+	+	0	+	0
	5	0	0	0	+	+	0	+	0
$[ZnCl_2(L)_2(H_2O)_2]{\cdot}3H_2O$	1	0	0	0	0	+	0	+	+
	2.5	0	0	0	0	+	0	+	+
	5	0	0	0	0	+	0	+	+
Standard[a]	1	++	++	+++	++	++	++	++	++
	2.5	+++	+++	+++	++	++	+++	+++	++
	5	+++	+++	+++	++	++	+++	+++	++

[a] Reference standard is chloramphenicol as standard antibacterial agent, terbinafin as standard antifungal agent

+ = Inhibition values = 0.1–0.5 mm beyond control; ++ = Inhibition values = 0.6–1.0 mm beyond control; +++ = Inhibition values = 1.1–1.5 mm beyond control; 0 = not detected

temperature range 30–220 °C may be attributed to the decomposition of 2HCl, $2H_2O$, and $C_4H_2Cl_2$ molecules. The activation energy is 45.60 kJ mol^{-1}. The remaining decomposition steps found within the temperature range 220–700 °C with an estimated mass loss of 41.54 (calcd. 41.34) and 29.19% (calcd. = 28.79%) are reasonably accounted for the removal of $C_{20}H_{19}Cl_2$ N_4O_2 and $C_{12}H_7Cl_4$ molecules as gases, respectively.

The TG curve of the Ni(II) (Fig. 2f) complex represents four decomposition steps as shown in Table 3. The first two step of decomposition within the temperature range 25–250 °C correspond to the loss of $4H_2O$, 2HCl, and $C_6H_3Cl_2$ molecules with a mass loss of 27.48% (calcd. 27.66%). The energy of activation for this dehydration steps are 33.66 and 49.901 kJ mol^{-1}. The third stage within the temperature range 250–400 °C which may be attributed to the loss of $C_{15}H_{14}Cl_2N_4O$ molecule with a mass loss of 32.04% (calcd. 32.40%). The subsequent step (400–700 °C) corresponds to the removal of $C_{15}H_{11}Cl_4O$ molecule leaving metal oxide as a residue. The overall weight loss amounts to 93.12% (calcd. 93.23%).

The DTA results are listed in Table 3 and represented graphically in Fig. 2. The appearance of many exothermic and endothermic peaks in the DTA (Table 3) can be attributed to the gaseous decomposition of the water, anions, and ligand molecules during decomposition process of the complexes [38].

Biological activity

Since the use of MCNZ drug as effective antifungal drug, the interest toward transition metal complexes containing *N*-donor ligands has increased in order to obtain metal-based drugs exhibiting a high biological activity together with a reduced toxicity. In this respect, in vitro biological activity of MCNZ drug with its transition metal complexes have been investigated. The data obtained shows that MCNZ drug under investigation and its metal complexes have the capacity of inhibiting the metabolic growth of the investigated bacteria and fungi to different extent. The size of the inhibition zone depends upon the culture medium, incubation conditions, rate of diffusion and the concentration of the antibacterial agent. The activities of all the tested complexes may be explained on the basis of chelation theory; chelation reduces the polarity of the metal atom mainly because of partial sharing of its positive charge with the donor groups and possible π electron delocalization within the whole chelate ring. Also, chelation increases the lipophilic nature of the central atom which subsequently favors its permeation through the lipid layer of the cell membrane.

In testing the antibacterial and antifungal activity of MCNZ drug and its metal complexes, more than one test organism is used to increase the chance of detecting antibiotic principles in tested materials. The sensitivity of a microorganism to antibiotics and other antimicrobial agents is determined by the assay plates which incubated at 28 °C for 2 days for yeasts and at 37 °C for 1 day for bacteria. All of the tested compounds show a remarkable biological activity against different types of fungi (*Aspergillus fumigatus*, *Penicillium italicum, Syncephalastrum racemosum, and Candida albicans*), Gram-positive bacteria (*Staphylococcus aureus, Pseudomonas aeruginosa*), and Gram-negative bacteria (*Bacillus subtilis, Escherichia coli*). The data are listed in Table 4. It is clear from the obtained results that:

(a) Using *A. fumigatus* and *P. italicum* fungi: The data listed in Table 4 shows that Cr(III) and Fe(III) complexes have the higher biological activity than that of the free drug while the Cu(II), Co(II), Mn(II), Ni(II), and Zn(II) drug complexes show no biological activity.
(b) Using *S. racemosum* fungus: It is clear from Table 4 that MCNZ and its metal complexes have no antifungal activity.
(c) Using *Candida albican* fungus: MCNZ and its metal complexes show moderate effect on this kind of fungus, The inhibition values are ranged from 0.1 to 1.0 mm beyond control. The data listed in Table 4 illustrate that the antifungal activity is found to follow the order: Mn(II) = Ni(II) > MCNZ > Co(II) = -Cu(II) > Cr(III), while Zn(II) and Fe(III) complexes are found to have no antifungal activity.
(d) Using *S. aureus* (G ± bacteria): It is obvious from the data listed Table 4 that MCNZ and its metal complexes have the same antibacterial activity.
(e) Using *P. aeruginosa* bacteria: The results also show that metal complexes of MCNZ drugs have no activity, but Cu(II), Co(II), Ni(II), Zn(II), and Fe(III) complexes of MCNZ have bacterial activity at higher concentrations (5 mg L^{-1}) only.
(f) Using *B. subtilis* bacteria: MCNZ and its metal complexes are found to have antibacterial activity against *B. subtillis* bacteria (an example of G^- negative bacteria), and the activity is found to have the order: Fe(III) > Ni(II) > MCNZ = Cu(II) = -Co(II) Mn(II) = Zn(II) = Cr(III).
(g) Using *E. coli* bacteria

It is clear that Zn(II) complex of MCNZ drug only show antibacterial activity against *E. Coli* (Table 4).

Structural interpretation

The structures of the complexes of MCNZ drug with Cr(III), Mn(II), Fe(III), Co(II), Ni(II), Cu(II), and Zn(II) ions are confirmed by the elemental analyses, IR, molar conductance, magnetic, solid reflectance, mass, and

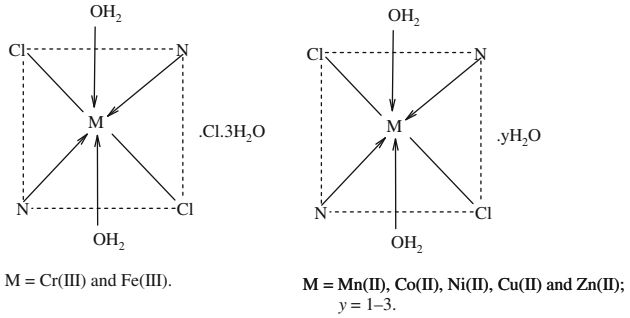

Fig. 3 Structures of metal complexes

thermal analyses (TG and DTA) data. Therefore, from the IR spectra, it is concluded that MCNZ drug behaves as a neutral undentate ligand coordinated to the metal ions via the imidazole-*N*. The molar conductance data, it is found that the bivalent complexes are non electrolytes while trivalent complexes are 1:1 electrolytes. On the basis of the above observations and from the magnetic and solid reflectance measurements, octahedral geometrical structure is suggested for the investigated complexes. As a general conclusion, the investigated MCNZ drug complexes structurs can be given as shown in Fig. 3.

References

1. Mascini M, Bagni G, Pietro MLD, Ravera M, Baracco S, Osella D. Electrochemical biosensor evaluation of the interaction between DNA and metallo-drugs. Biometals. 2006;19:409–18.
2. Kostova I. Platinum complexes as anticancer agents. Recent Pat Anti-Cancer Drug Discov. 2006;1:1–22.
3. Guo Z, Sadler PJ. Advances in inorganic chemistry, vol. 49. San Diego: Academic Press; 2000. p. 183–306.
4. Davis H Jr, Lake CM, Bernard MA. Azolidene carbenes derived from biologically relevant molecules. 1. Synthesis and characterization of iridium complexes of imidazolidene ligands based upon the antifungal drugs econazole and miconazole. Inorg Chem. 1998;37:5412–3.
5. Roth HJ, Kleeman A. Pharmaceutical chemistry. New York: John Wiley; 1988. p. 218.
6. Joule JA, Mills K, Smith GF. Heterocyclic chemistry. 3rd ed. New York: Chapman & Hall; 1995.
7. Arduengo AJIII, Harlow RL, Kline M. A stable crystalline carbene. J Am Chem Soc. 1991;113:361–3.
8. Arduengo AJ III, Dias HVR, Harlow RL, Klooster WT, Koetzle TF. Electron distribution in a stable carbene. J Am Chem Soc. 1994;116:6812–22.
9. Alder RW, Allen PR, Williams SJ. Stable carbenes as strong bases. J Chem Soc Chem Commun; 1995. p. 1267–1268.
10. Breslow R. Rapid deuterium exchange in thiazolium salts. J Am Chem Soc. 1957;79:1762–3.
11. Breslow R. On the mechanism of thiamine action. IV. Evidence from studies on model system. J Am Chem Soc. 1958;80:3719–26.
12. Wanzlick H-W, Schönherr H. Direct synthesis of a mercury salt-carbene complex. J Angew Chem Int Ed Engl. 1968;7:141–2.
13. Ofele K. 1,3-Dimethyl-4-Imidazolinyliden-92-pentacarbonylchromein neuer ubeergangsmetall-carbene-komplex. J Organomet Chem. 1968;12:42–3.
14. Herrmann WA, Kocher C. N-heterocyclic carbenes. Angew Chem Int Ed Engl. 1997;36:2162–87.
15. Transmethylation: Proceedings of the Conference on Transmethylation, Bethesda, Maryland, U.S.A., on October 16–19, 1978. In: Usdin E, Borchardt T, Creveling CR, editors. Developments in Neuroscience, vol. 5. New York: Elsevier/North Holland; 1979.
16. Razin A, Cedar H, Riggs AD, editors. DNA methylation: biochemistry and biological significance (Springer series in molecular biology). New York: Springer Verlag; 1984.
17. Mangas-Snchez J, Busto E, Gotor-Fernndez V, Malpartida F, Gotor V. Asymmetric chemoenzymatic synthesis of miconazole and econazole enantiomers. The importance of chirality in their biological evaluation. J Org Chem. 2011;76:2115–22.
18. Bray MR, Deeth RJ. Computer modeling of electron paramagnetic resonance-active molybdenum(V)species in xanthine oxidase. J Chem Soc Dalton Trans; 1997. p. 4005–10.
19. Farrell N. Inorganic complexes as drugs and chemotherapeutic agents. In: McCleverty JA, Meyer TJ, editors. Comprehensive coordination chemistry, vol. 9. 2nd ed. Oxford: Elsevier Pergamon; 2004. p. 809–40.
20. Clement JL, Jarret PS. Antibacterial silver. Met Based Drugs. 1994;1:467–82.
21. Tambe SM, Sampath L, Modak SM. In vitro evaluation of the risk of developing bacterial resistance to antiseptics and antibiotics used in medical devices. J Antimicrob Chemother. 2001;47:589–98.
22. Jakupec MA, Unfried P, Keppler BK. In vitro evaluation of the risk of developing bacterial resistance to antiseptics and antibiotics used in medical devices. Rev Physiol Biochem Pharmacol. 2005;153:101–11.
23. Nomiya K, Takahashi S, Noguchi R, Nemoto S, Takayama T, Oda M. Synthesis and characterization of water-soluble silver(I) complexes with L-histidine (H2his) and (S)-(−)-2-pyrrolidone-5-carboxylic acid (H2pyrrld) showing a wide spectrum of effective antibacterial and antifungal activities. Crystal structures of chiral helical polymers [Ag (Hhis)] n and [Ag (Hpyrrld)] 2n in the solid state. Inorg Chem. 2000;39:3301–11.
24. Kasuga NC, Sugie A, Nomiya K. Syntheses, structures and antimicrobial activities of water soluble silver(I)–oxygen bonding complexes with chiral and racemic camphanic acid (Hca) ligands. Dalton Trans. 2004. p. 3732–3740.
25. Özdemir İ, Özge Özcan E, Günal S, Gürbüz N. Synthesis and antimicrobial activity of novel Ag-N-hetero-cyclic carbene complexes. Molecules. 2010;15:2499–508.
26. Abu-Salah KM. Amphotericin B: an update. Brit J Biomed Sci. 1996;53:122–33.
27. Canuto M, Rodero FG. Antifungal drug resistance to azole and polyenes. Lancet (Infect Dis). 2002;2:550–62.
28. Eshwika A, Coyle B, Devereux M, McCann M, Kavanagh K. Metal complexes of 1,10-phenanthroline-5,6-dione alter the susceptibility of the yeast *Candida albicans* to Amphotericin B and Miconazole. BioMetals; 2004.17:415–422.
29. Sanchez-Delgado RA, Lazardi K, Rincon L, Urbina JA. Toward a novel metal-based chemotherapy against tropical diseases. 1. Enhancementof the efficacy of clotrimazole against *Trypanosoma Cruzi* by complexation to ruthenium in $RuCl_2$(clotrimazole)$_2$. J Med Chem. 1993;36:2041–3.
30. Sanchez-Delgado RA, Perez H, Urbina JA. Toward a novel metal-based chemotherapy against tropical diseases. 2. Synthesis and antimalarial activity in vitro and in vivo of the new ruthenium and rhodium-chloroquine complex. J Med Chem. 1996;39:1095–9.

31. Sanchez-Delgado RA, Perez H, Navarro. Toward a novel metal-based chemotherapy against tropical diseases. 3. Synthesis and antimalarial activity in vitro and in vivo of the new gold-chloroquine complex[Au(PPh_3)(CQ)]PF_6;M. J Med Chem. 1997;40:1937–9.
32. Soliman MH, Mohamed GG, Mohamed AE. Metal complexes of Fenoterol drug. Preparation, spectroscopic, thermal and biological activity characterization. J Therm Anal Calorim. 2010;99: 639–47.
33. Mohamed GG, Soliman MH. Synthesis, spectroscopic and thermal characterization of sulpiride complexes of iron, manganese, copper, cobalt, nickel, and zinc salts. Antibacterial and antifungal activity. Spectrochim Acta A. 2010;76:341–7.
34. Cotton FA, Wilkinson G, Murillo CA, Bochmann M, Chemistry AdvancedInorganic. 6. New York: Wiley; 1999.
35. Mohamed GG, Badawy MA, Omar MM, Nassar MM, Kamel AB. Synthesis, spectroscopic, thermal and biological activity studies on triazine metal complexes. Spectrochim Acta A. 2010;77: 773–81.
36. Mohamed GG, Zayed MA, Abdallah SM. Metal complexes of a novel Schiff base derived from sulphametrole and varealdehyde. Synthesis, spectral, thermal characterization and biological activity. J Mol Str. 2010;979(1–3):62–71.
37. Biswas S, Mitra K, Schwalbe CH, Lucas CR, Chattopadhyay SK, Adhikary B. Synthesis and characterization of some Mn(II) and Mn(III) complexes of N,N′-o-phenylene-bis(salicylideneimine) (LH2) and N,N′-o-phenylenebis(5-bromo-salicyliden-eimine) (L′H2). Crystal structures of [Mn(L)(H2O)(ClO4)], [Mn(L) (NCS)] and an infinite linear chain of [Mn(L)(OAc)]. Inorg Chim Acta. 2005;358:2473–81.
38. Refat SM, Mohamed GG, de Farias FR, Powell KA, El-Garib SM, El-Korashy AS, Hussien AM. Spectroscopic and thermal studies of different anions of Zn(II), Cd(II) and Hg(II) with norfloxacin drug. J Therm Anal Calorim. 2010;102:225–32.